*Journal of Sound and Vibration* (2002) **250**(2), 356–367
doi:10.1006/jsvi.2001.3725, available online at http://www.idealibrary.com on IDEAL®

# STABILITY ANALYSIS OF SPINNING STEPPED-SHAFT WORKPIECES IN A TURNING PROCESS

Z. C. Wang and W. L. Cleghorn

*Department of Mechanical and Industrial Engineering, University of Toronto, Toronto, Ont, Canada M5S 3G8*

(*Received* 6 *June* 2000, *and in final form* 4 *May* 2001)

## 1. INTRODUCTION

Metal cutting process is often accompanied by a violent vibration between the workpiece and the cutting tool. This type of vibration is called chatter. Chatter of large amplitude may generate high-pitch noise, cause poor surface finish, tool wear, tool fracture and damage to the machine tool system. Chatter is a critical factor that limits productivity. To avoid chatter, metal removal rate has to be reduced to maintain chatter-free operation. Modelling and analysis of the machine tool system for chatter are important to achieve high quality and high productivity.

A chatter model consists of mathematical formulations of the cutting force and the motion of the dynamic system including the workpiece and cutting tool. In stability analysis, we will determine the critical cutting conditions in terms of cutting speed, feed rate and cutting depth under which chatter occurs. Since the 1940s, a large amount of research has been done to investigate chatter phenomena. Cutting force models have been investigated by many researchers. General static cutting force models are shear plane model, slip line model, and shear zone model. Among them, Merchant's shear plane model [1] has been widely used to investigate the effects of process geometry, shear-zone size, strain rate and temperature on cutting force.

Lee and Shaffer [2] introduced plasticity into the cutting force model. Wu and Liu [3] proposed a modified model to determine dynamic cutting force in a turning process. This model can be used to explain the following three types of chatter: Arnold-type chatter, regenerative chatter, and mode-coupling chatter. Based on the model of Wu and Liu, Minis and Tembo [4] provided a set of cutting force equations to describe the variation of the cutting force as a function of the change in the inner and outer chip surface shape. In stability analysis, the cutting force is usually assumed to be proportional to the cross-sectional area of the chip for steady state cutting. The simplest dynamic cutting force model assumes that the cutting force is proportional to the instantaneous depth of cut.

Merritt [5] described chatter theory using a feedback loop for stability analysis of the cutting process. In Merritt's chatter model, the workpiece is simplified into a lumped system with one or many degrees of freedom; the cutting force is assumed to be proportional to the instantaneous uncut chip thickness. The feedback loop consists of a primary feedback path and a regenerative feedback path. In Merritt's theory, an overlap factor is introduced to account for the portion of the previous cut that overlaps the present cut. If the overlap

0022-460X/02/070356 + 12 $35.00/0 

factor is zero, the chatter is termed as primary chatter; otherwise, it is termed as regenerative chatter.

Kato and Marui [6] investigated the causes of regenerative chatter due to workpiece deflection in a cutting process. They performed cutting experiments using mild steel and cast iron under steady cutting conditions. A square thread was cut on an iron workpiece to investigate the regenerative effect. They concluded that the regenerative effect is the main cause of chatter. Based on the experiments, they developed a simplified chatter model in which the workpiece is considered as a single-degree-of-freedom system and the cutting force is considered to be proportional to the chip load.

As a workpiece is constrained by the chuck and the tailstock, a realistic description of boundary conditions in the chatter model is critical to an accurate prediction of chatter onset. In the 1980s, the workpiece was usually modelled as a lumped mass with springs and dampers attached to it [7, 8]. Significant contributions to the workpiece model were made by Lu and Klamecki [9]. They modelled a slender workpiece as a uniform Euler beam with two types of boundary conditions. In their work, the chuck is modelled as a rotational spring attached to a hinge at one end of the workpiece; the tailstock is modelled as a translational spring attached to the other end. The cutting force is considered to be proportional to the instantaneous depth of cut. A number of chatter experiments were performed on mild steel shafts with different dimensions under various cutting conditions. The experimental results showed good agreement with the theoretical predictions.

Stability conditions are usually expressed in a stability chart. Various methodologies have been used to obtain a stability chart. Lin [10] investigated the stability of a lumped mass system using an analytical method. The author separated the characteristic equation of this system into a real part and an imaginary part in the frequency domain. The chatter frequencies and critical cutting conditions were obtained analytically. Hwang *et al.* [11] used a limit cycle to determine the stability in the time domain.

Many researchers have used the gain-phase plot to obtain a stability chart. Intersection of the dynamic compliance with the points on the critical loci gives harmonic solutions of the characteristic equation, which define the boundaries of stability. Another method to obtain a stability chart is the gain-factor method. Chen *et al.* [12, 13] and Wang *et al.* [14] plotted the Nyquist plot and used the gain-factor method to obtain the critical cutting conditions from the intersection of the non-zero term of the characteristic equation with the real axis. The advantage of this method is that the critical cutting conditions and the chatter frequencies can be obtained directly.

Up to now, the workpiece has been modelled either as a lumped mass, with which it is difficult to describe the true behavior of the workpiece and to incorporate realistic boundary conditions; or as a uniform beam, which is valid only for a uniform cross-section workpiece. In the chatter model of a workpiece, incorporation of the effects of rotary inertia and transverse shear deformations are necessary as many workpieces are spinning at very high speed and have a low length-to-diameter ratio. Unfortunately, these factors are not reflected in the literature; the spinning workpiece is considered non-spinning; gyroscopic effects are neglected; and only Euler beam theory is applied. In industry, the cross-section of workpiece is often non-uniform. Stepped-shaft workpieces, for example, are commonly encountered in a turning process.

The objectives of this paper are to develop a mathematical model of spinning stepped-shaft workpiece, and to perform a stability analysis. A two-node, 16-degree-of-freedom Timoshenko beam finite element is used. The cutting force is assumed to be proportional to the instantaneous depth of cut. Nyquist stability criterion is applied and the gain-factor method is adopted to determine the stable conditions. The

predicted onset conditions of chatter are compared with the experimental data obtained by other researchers.

## 2. CHATTER MODEL

### 2.1. STEPPED-SHAFT WORKPIECE MODEL

As shown in Figure 1, a stepped-shaft workpiece is supported by a chuck and a tailstock at the two ends. The boundary conditions at the chuck end are simple support plus two rotational springs. The boundary conditions at the tailstock end are free plus two translational springs. Using the finite element method, the workpiece is divided into a number of uniform Timoshenko beam elements. Within each element, the equations of motion for a spinning beam may be written as [15]

$$\rho A\frac{\partial^2 u_x}{\partial t^2} - \kappa GA\left(\frac{\partial^2 u_x}{\partial z^2} - \frac{\partial \phi_x}{\partial z}\right) + c_d\frac{\partial u_x}{\partial t} = F_x[u_c(t-\tau),\quad u_c(t)]\,\delta(z-z_c),$$

$$\rho A\frac{\partial^2 u_y}{\partial t^2} - \kappa GA\left(\frac{\partial^2 u_y}{\partial z^2} - \frac{\partial \phi_y}{\partial z}\right) + c_d\frac{\partial u_y}{\partial t} = F_y[u_c(t-\tau),\quad u_c(t)]\,\delta(z-z_c),$$

$$-EI\frac{\partial^2 \phi_x}{\partial z^2} - \kappa GA\left(\frac{\partial u_x}{\partial z} - \phi_x\right) + \rho I\left(\frac{\partial^2 \phi_x}{\partial t^2} + 2\Omega\frac{\partial \phi_y}{\partial t}\right) = 0,$$

$$-EI\frac{\partial^2 \phi_y}{\partial z^2} - \kappa GA\left(\frac{\partial u_y}{\partial z} - \phi_y\right) + \rho I\left(\frac{\partial^2 \phi_y}{\partial t^2} - 2\Omega\frac{\partial \phi_x}{\partial t}\right) = 0, \tag{1}$$

where $\rho$ is the mass density of the beam material, $G$ is the shear modulus, $E$ is the modulus of elasticity, $A$ is the cross-section area, $I$ is the second moment of area, $\kappa$ is the shear-correction factor, $c_d$ is the equivalent viscous damping coefficient, $\Omega$ is the spin rate of the workpiece, $u_x$ and $u_y$ are lateral displacements of the beam in the $x$ and $y$ directions respectively, $\phi_x$ and $\phi_y$ are bending angles in the $xoz$ and $yoz$ planes respectively, $u_c$ is the lateral displacement at the cutting point in the $x$ direction, $\tau$ is the period of one revolution of the workpiece, $\tau = 2\pi/\Omega$, $F_x$ and $F_y$ are cutting forces acting on the workpiece in the $x$ and $y$ directions, respectively, and they are functions of the displacement $u_c$ at the cutting

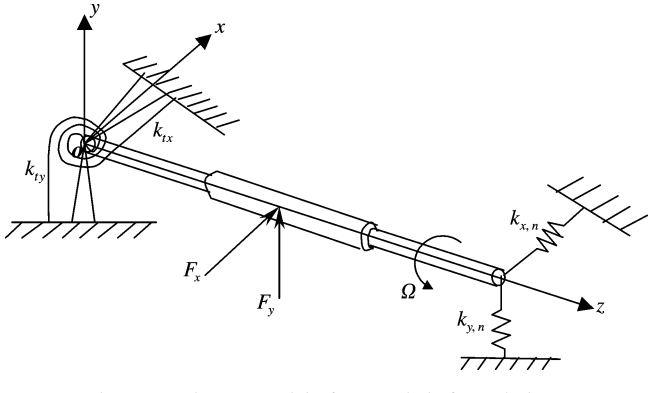


Figure 1. Chatter model of stepped-shaft workpiece.

point, $\delta$ is the Dirac delta function, and $z_c$ is the co-ordinate of the cutting point in the $z$ direction.

Assuming that the lateral displacements and bending angles vary cubically along the $z$-axis, a two-node, 16-degree-of-freedom Timoshenko beam element can be used. Using this type of element, the global equations of motion for a spinning stepped-shaft workpiece may be written as

$$\mathbf{M}\ddot{\mathbf{q}} + \mathbf{G}\dot{\mathbf{q}} + \mathbf{K}\mathbf{q} = \mathbf{Q}, \tag{2}$$

where **M**, **G**, and **K** are global mass, gyroscopic and stiffness matrices respectively, **q** is the global nodal displacement vector, and **Q** is the force vector.

In the state space, the second order dynamic system can be reduced to an equivalent first order dynamic system using the transformation

$$\mathbf{p} = \dot{\mathbf{q}}. \tag{3}$$

Equation (2) may be written as

$$\mathbf{D}_2\dot{\mathbf{X}} = \mathbf{D}_1\mathbf{X} + \mathbf{D}_0, \tag{4}$$

where

$$\mathbf{X} = \begin{Bmatrix} \mathbf{q} \\ \mathbf{p} \end{Bmatrix}, \quad \mathbf{D}_2 = \begin{bmatrix} \mathbf{I} & \mathbf{0} \\ \mathbf{0} & \mathbf{M} \end{bmatrix}, \quad \mathbf{D}_1 = \begin{bmatrix} \mathbf{0} & \mathbf{I} \\ -\mathbf{K} & -\mathbf{G} \end{bmatrix}, \quad \mathbf{D}_0 = \begin{Bmatrix} \mathbf{0} \\ \mathbf{Q} \end{Bmatrix}.$$

## 2.2. CUTTING FORCE MODEL

In a steady state cutting process, the cutting force is proportional to the cross-sectional area. The cutting process can be expressed using a regenerative feedback loop shown in Figure 2. A simple cutting force model according to Lu and Klamecki [9] is

$$F_x = k_x u(t), \quad F_y = k_y u(t), \tag{5, 6}$$

where $k_x$ and $k_y$ are the static cutting stiffness in the $x$ and $y$ directions, respectively, and the instantaneous depth of cut $u(t)$ as shown in Figure 3 is

$$u(t) = u_0 + \mu u_c(t - \tau) - u_c(t), \tag{7}$$

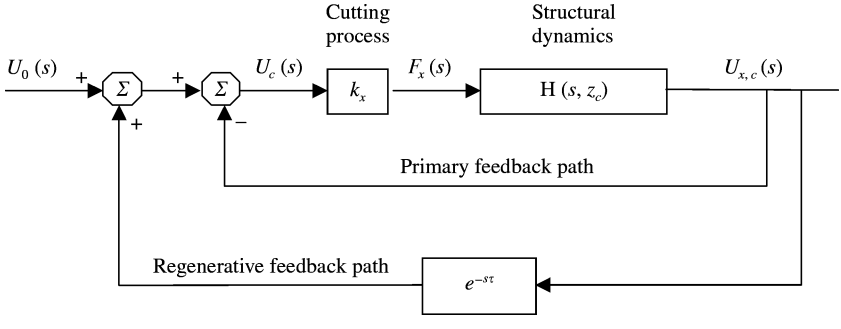


Figure 2. Feedback loop of cutting process.

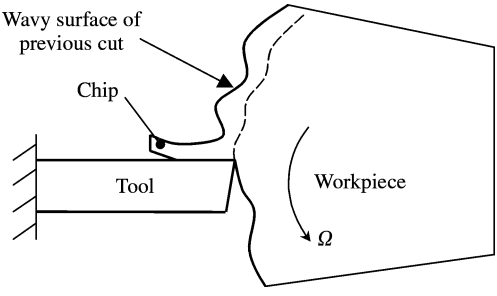


Figure 3. Schematic view of a cutting process.

where $u_0$ is the nominal depth of cut, $\mu$ is the overlap factor. The nominal cutting depth $u_0$ does not play a role in the dynamic cutting force and will not be included in the dynamic cutting force expression.

Incorporating equations (5)–(7) into the global load vector in equation (2), the global force vector due to the dynamic cutting force may be written as

$$\mathbf{Q} = \begin{bmatrix} 0 \\ \vdots \\ F_x \\ 0 \\ 0 \\ 0 \\ F_y \\ \vdots \\ 0 \end{bmatrix} = \begin{bmatrix} 0 \\ \vdots \\ k_x[\mu u_c(t-\tau) - u_c(t)_x] \\ 0 \\ 0 \\ 0 \\ k_y[\mu u_c(t-\tau) - u_c(t)] \\ \vdots \\ 0 \end{bmatrix} \begin{matrix} \\ \\ \leftarrow [8(n_c-1)+1], \\ \\ \\ \\ \leftarrow [8(n_c-1)+5], \\ \\ \end{matrix} \tag{8}$$

where $n_c$ is the node number of the cutting point. The right-hand side of equation (2) is modified accordingly. So the modified equation (4) can be rewritten as

$$\mathbf{D}_2\dot{\mathbf{X}} = \mathbf{D}_1\mathbf{X} + \mathbf{D}, \tag{9}$$

where $\mathbf{D} = [\mathbf{0} \quad \mathbf{Q}^{\mathrm{T}}]^{\mathrm{T}}$, matrix $\mathbf{K}$ and matrix $\mathbf{D}_1$ are subjected to the modifications for boundary conditions. The stability analysis is taken in the Laplace domain. The Laplace transforms of the cutting force components are

$$\bar{F}_x(s) = k_x\lfloor \mu e^{-\tau s}U_c(s) - U_c(s) \rfloor, \quad \bar{F}_y(s) = k_y[\mu e^{-\tau s}U_c(s) - U_c(s)]. \tag{10, 11}$$

The transfer function of the regenerative feedback system is defined as

$$T_r = \frac{U_c(s)}{U_0(s)}, \tag{12}$$

where $\bar{F}_x(s)$ and $\bar{F}_y(s)$ are the Laplace transforms of $F_x$ and $F_y$ respectively, $U_c(s)$ and $U_0(s)$ are the Laplace transforms of $u_c$ and $u_0$ respectively.

## 3. STABILITY ANALYSIS

According to the mode superposition theory, we assume a solution to equation (9) in the form

$$\{X\} = \sum_{i=-2N}^{2N} \{\bar{X}\}_i g_i(t), \tag{13}$$

where the positive values of $i$ implicitly indicate the forward precession, the negative values of $i$ correspond to backward precession, $N$ is the order of mode truncation, $\{\bar{X}\}_i$ is the $i$th eigenvector of the dynamic system, and $g_i(t)$ is the generalized co-ordinate. In state space, there are two forward vibration modes and two backward vibration modes. For each mode of vibration, the two forward modes are complex and conjugates of each other; and the two backward modes are complex and conjugates of each other. The dynamic system is not self-adjoint because of the gyroscopic effect [16]. To solve the eigenvalue problem of a non-self-adjoint system, we define an adjoint system

$$[D_2^*]\,\dot{\mathbf{Y}} = [D_1^*]\,\mathbf{Y}, \tag{14}$$

where $\mathbf{Y}$ is the state vector of the adjoint system, and

$$[D_2^*] = [D_2]^{\mathrm{T}}, \quad [D_1^*] = [D_1]^{\mathrm{T}}.$$

Multiplying equation (4) on the left by $\{\bar{Y}\}_i^{\mathrm{T}}$, and applying the biorthogonal relationships between the original and the adjoint systems, we obtain

$$a_i \dot{g}_i(t) = b_i g_i(t) + \{\bar{Y}\}_i^{\mathrm{T}} \mathbf{D}, \quad i = \pm 1, \pm 2, \ldots, \pm 2N, \tag{15}$$

where $a_i$ and $b_i$ are scalars, $\{\bar{Y}\}_i$ is the $i$th eigenvector of the adjoint system. Substituting equations (5) and (6) into the above equation and taking the Laplace transform, assuming zero initial conditions, we obtain

$$a_i s G_i(s) = b_i G_i(s) + \bar{Y}_{x,i} F_x(s) + \bar{Y}_{y,i} F_y(s), \quad i = \pm 1, \pm 2, \ldots, \pm 2N, \tag{16}$$

where $\bar{Y}_{x,i}$ is element $[n + 8(n_c - 1) + 1]$ of eigenvector $\{\bar{Y}\}_i$, $\bar{Y}_{y,i}$ is element $[n + 8(n_c - 1) + 5]$ of eigenvector $\{\bar{Y}\}_i$. Equation (14) can be expressed as

$$a_i s G_i(s) = b_i G_i(s) + (\bar{Y}_{x,i} + c\bar{Y}_{y,i}) k_x (\mu \mathrm{e}^{-s\tau} - 1) \sum_{j=-2N}^{2N} \bar{X}_{nc,j} G_j(s), \tag{17}$$

where $G_i(s)$ is the Laplace transform of $g_i(t)$, constant $c = k_y/k_x$, and $\bar{X}_{nc,j}$ is element $[n + 8(n_c - 1) + 1]$ of the eigenvalue vector $\{\bar{X}\}_i$ corresponding to the cutting point. From equation (17),

$$G_i(s) = \frac{(a_1 s - b_i)(\bar{Y}_{x,i} + c\bar{Y}_{y,i})}{(a_i s - b_i)(\bar{Y}_{x,1} + c\bar{Y}_{y,1})} G_1(s), \quad i = \pm 1, \pm 2, \ldots, \pm 2N. \tag{18}$$

From equations (5)–(7), we can obtain the relation between $U_0(s)$ and $U_c(s)$. From equations (13) and (18), we obtain

$$\frac{U_c(s)}{U_0(s)} = \sum_{i=-2N}^{2N} k_x \bar{X}_{nc,i} \frac{(a_1 s - b_1)(\bar{Y}_{x,i} + c\bar{Y}_{y,i})}{(a_i s - b_i)(\bar{Y}_{x,1} + c\bar{Y}_{y,1})} \frac{G_1(s)}{U_0(s)} (\mu \mathrm{e}^{-s\tau} - 1). \tag{19}$$

The characteristic equation is

$$(a_1 s - b_1)(a_2 s - b_2) \cdots (a_{2n} s - b_{2n}) \left[ 1 - k_x \sum_{i=-2N}^{2N} X_{u,i} \frac{(\bar{Y}_{x,i1} + c\bar{Y}_{y,i})}{(a_i s - b_i)} (\mu e^{-s\tau} - 1) \right] = 0. \tag{20}$$

Examination of the above equation indicates that regenerative chatter occurs when the following conditions are satisfied:

$$1 - k_x \sum_{i=-2N}^{2N} X_{nc,i} \frac{(\bar{Y}_{x,i1} + c\bar{Y}_{y,i})}{(a_i s - b_i)} (\mu e^{-s\tau} - 1) = 0 \tag{21}$$

or

$$1 - k_x H(s, z_c)(\mu e^{-s\tau} - 1) = 0, \tag{22}$$

where

$$H(s, z_c) = \sum_{i=-2N}^{2N} X_{nc,i} \frac{(\bar{Y}_{x,i1} + c\bar{Y}_{y,i})}{(a_i s - b_i)}.$$

The solution of this non-linear algebraic equation determines the chatter onset conditions of the cutting process.

## 4. NUMERICAL EXAMPLES

In order to illustrate the procedure of a stability analysis, a uniform shaft and a two-segment stepped shaft are investigated. In these two examples, the workpiece is simply supported and is attached to rotational springs at the end of the chuck. The other end of the workpiece is free. Because the effect of higher mode on the stability is very small, we retain only the first two modes of vibration, i.e., $N = 2$ in equation (21).

For a given cutting tool position along the workpiece, chatter may occur when the cutting conditions change. Chatter may also occur when the cutting conditions remain the same but the cutting tool moves along the workpiece. These two cases are investigated for uniform shafts. For the stepped shaft, the critical stability conditions are investigated for a given cutting tool position along the workpiece.

For the purpose of comparison, a uniform shaft is first investigated. This problem was studied by Lu [9]. First, we will predict the critical cutting conditions when the cutting tool is at the middle of the workpiece. Then, we will predict the tool location at which the cutting process changes from stable cutting state to chatter when the cutting tool moves from the chuck to the free end of the workpiece. The values of parameters pertinent to the workpiece and cutting process are given as

$$\rho = 7700\,\text{kg/m}^3, \quad E = 207\,\text{GPa}, \quad G = 77.6\,\text{GPa}, \quad \kappa = 0{\cdot}9, \quad \mu = 1, \quad l = 0{\cdot}381\,\text{m},$$

$$d = 0{\cdot}035\,\text{m}, \quad k_x = 124\,367\,\text{N/m}, \quad k_{tx} = 84\,032\,\text{N m/rad}.$$

In this paper, the rotational stiffness $k_{ty}$ is assumed to be the same as $k_{tx}$, and the cutting stiffness $k_y$ is also assumed to be the same as $k_x$. The Nyquist stability criterion requires that the roots of equation (22) be confined to the left half of the $s$-plane. Substituting $s = j\omega$ into

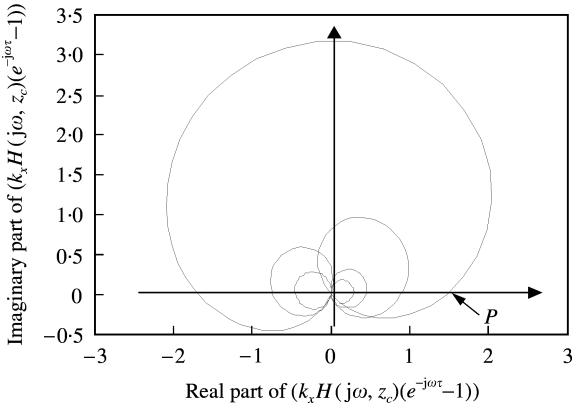


Figure 4. Nyquist plots.

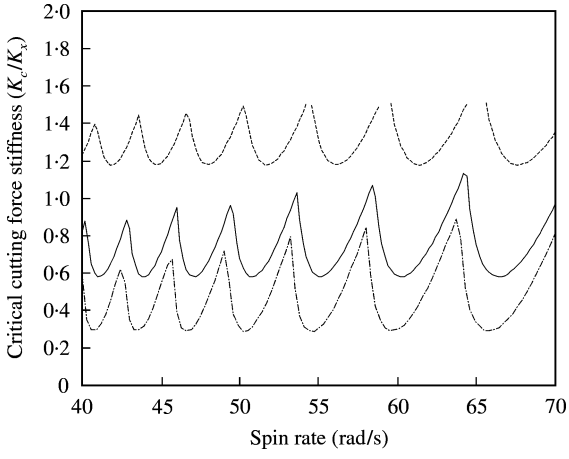


Figure 5. Stability chart of the uniform shaft: ·····, $\varsigma = 0{\cdot}01$; ——, $\varsigma = 0{\cdot}02$; - - - -, $\varsigma = 0{\cdot}04$.

equation (22), where $\omega$ is the chatter frequency, we will examine the encirclement of the point $(1 + j0)$ by the $k_x H(j\omega, z_c)(\mu e^{-j\omega\tau} - 1)$ loci. The presence of the time-delay term in the characteristic equation leads to multiple intersections of the plot with the real axis as shown in Figure 4. Let $P$ be the co-ordinate of the right-most intersection point between the Nyquist contour of the term $k_x H(j\omega, z_c)(\mu e^{-j\omega\tau} - 1)$ and the real axis. The closed-loop system is stable if $P > 1$, unstable if $P < 1$, and critical if $P = 1$. Under a specific cutting condition, the right-most intersection point of the open-loop locus is at $P$. By changing the cutting force stiffness $k_x$ or the location of the cutting point $z_c$, we can obtain the critical cutting condition at which the open-loop loci will pass through point $(1 + j0)$. Using this approach, the limit of critical stability conditions can be determined.

The equivalent damping coefficient $c_d$ is calculated from the equivalent damping ratio $\varsigma$. Values of damping ratio are selected to be 0·01, 0·02, and 0·04. A stability chart is plotted in Figure 5. In this case, the cutting tool is at the middle of the workpiece. We can see that the stability of the system is influenced by the spin rate. The critical cutting force parameter $k_x$ behaves like a periodic function of spin rate.

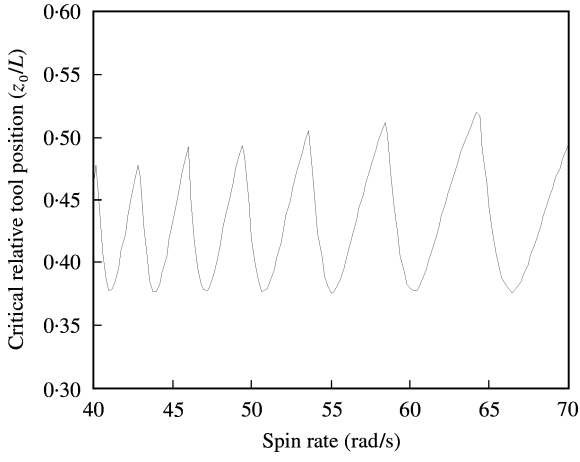


Figure 6. Critical relative tool position along the shaft from the chuck.

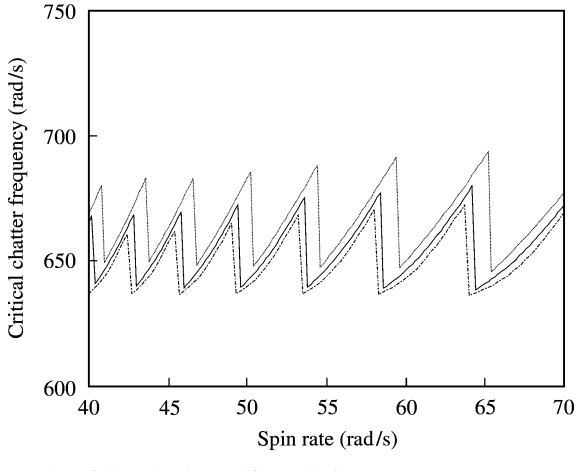


Figure 7. Chatter frequencies of the spinning uniform shaft: -·-·-·-, $\varsigma = 0{\cdot}01$; ——, $\varsigma = 0{\cdot}02$; - - - - -, $\varsigma = 0{\cdot}04$.

A stability chart is plotted for critical tool locations in Figure 6. The damping ratio is 0·02. In this case, the cutting conditions remain the same, but the cutting tool moves from the chuck to the tailstock along the workpiece. If the tool moves beyond the critical position, the system becomes unstable. Otherwise, the system is stable. Figure 7 shows the corresponding critical chatter frequency that occurs at the stability threshold. In this case, the cutting tool is at the middle of the workpiece. It is found that the corresponding chatter frequency increases with spin within each stability lobe.

A two-segment stepped shaft is investigated in this paper. For segment one, the diameter is $D1 = 0{\cdot}035$ m and the length is 0·127 m; for segment two, the diameter is $D2 = 0{\cdot}025$ m and the length is 0·254 m. The given cutting conditions and material properties remain the same. The chuck supports the end of segment one; and the end of segment two is free. The rotational spring stiffness $k_{tx} = 84032$ N m/rad, and $k_{ty} = k_{tx}$. The relative cutting tool location $z_c/L = 2/3$ from the chuck end. The damping ratio is 0·02. Figure 8 shows the

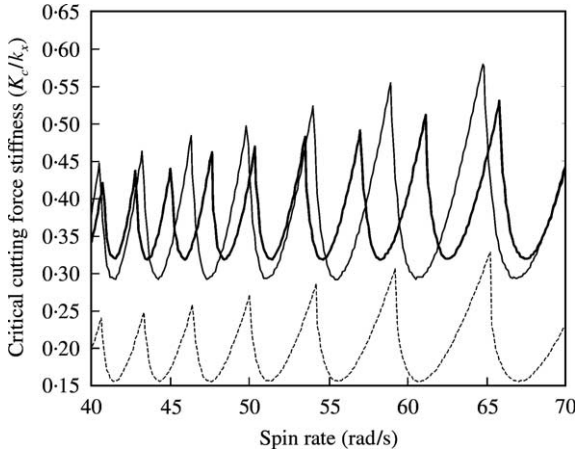


Figure 8. Stability charts of the stepped and uniform shafts: ——, stepped shaft, $D1 = 0{\cdot}035$ m, $D2 = 0{\cdot}025$ m; ——, uniform shaft, $D = 0{\cdot}035$ m; - - - - -, uniform shaft, $D = 0{\cdot}025$ m.

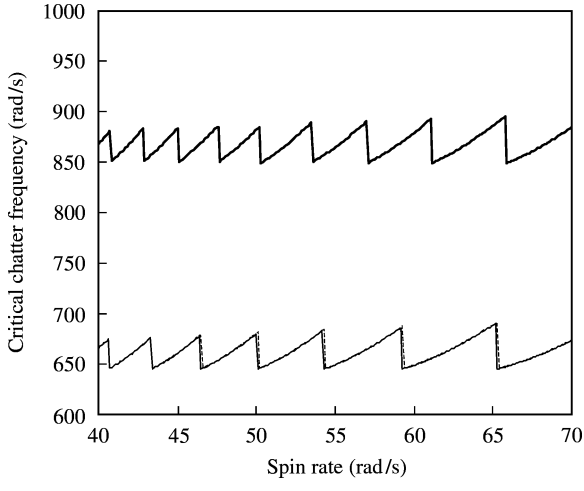


Figure 9. Chatter frequencies of the stepped and uniform shafts: ——, stepped shaft, $D1 = 0{\cdot}035$ m, $D2 = 0{\cdot}025$ m; ——, uniform shaft, $D = 0{\cdot}035$ m; - - - - -, uniform shaft, $D = 0{\cdot}025$ m.

stability charts and Figure 9 represents the critical chatter frequencies. With the same boundary conditions and cutting tool locations, the stability and chatter frequency charts of the uniform shaft with diameter $D = 0{\cdot}035$ m and another uniform shaft with diameter $D = 0{\cdot}025$ m are also presented in Figures 8 and 9. Figure 8 indicates that chatter will occur for all the stepped and uniform shafts at the given cutting tool location under the present cutting conditions. The natural frequencies of the uniform and stepped shafts are presented in Table 1. We can see that the first natural frequency of the stepped shaft is higher than that of the two uniform shafts. From Figures 6, 9 and Table1, we also find that the critical chatter frequency of a shaft is just above its first natural frequency. The critical chatter frequencies and stability chart are affected significantly by the workpiece geometry.

TABLE 1

*Natural frequencies of the uniform and stepped shafts with one end supported by a chuck and the other free (rad/s)*

| Mode | 1 | 2 | 3 | 4 |
|---|---|---|---|---|
| Uniform shaft ($D = 35$ mm) | 639·1 | 5200·6 | 15366·6 | 30069·7 |
| Stepped shaft ($D1 = 35$ mm, $D2 = 25$ mm) | 837·6 | 4198·0 | 13017·4 | 25218·3 |
| Uniform shaft ($D = 25$ mm) | 640·3 | 4225·7 | 12134·6 | 24092·2 |

TABLE 2

*Comparison of predicted chatter-onset locations with the experimental results* [9] *for uniform workpiece*

| Diameter (m) | Length (m) | Spring stiffness (Nm/rad) | Cutting stiffness (N/m) | Spin rate (rad/s) | Experimental value [9] $(z_c/L)_p$ | Predicted value $(z_c/L)_a$ | Error (%) |
|---|---|---|---|---|---|---|---|
| 0·0350 | 0·381 | 82351 | 124367 | 51·2 | 0·434 | 0·4043 | − 6·9 |
| 0·0381 | 0·381 | 86842 | 124367 | 51·2 | 0·466 | 0·4340 | − 6·8 |
| 0·0445 | 0·381 | 88610 | 124367 | 51·2 | 0·500 | 0·5192 | 3·8 |
| 0·0381 | 0·381 | 86150 | 156773 | 51·2 | 0·428 | 0·4059 | − 5·2 |

The predicted chatter-onset conditions for the above given cutting conditions are compared with the results of the experiments conducted by Lu and Klamecki. The results are listed in Table 2. The rotational spring stiffness and the cutting stiffness are taken from the work of Lu [17]. The difference between the predicted tool distance and the experimental results are within 7 per cent.

## 5. CONCLUSIONS

A chatter model of a spinning stepped-shaft workpiece has been developed using Timoshenko beam theory. Stability analysis of the dynamic system is performed using the finite element method, mode superposition method and the Laplace transformation. The roots of the non-linear characteristic equation are obtained using the Matlab program. Numerical simulations performed on uniform and stepped workpieces indicate that chatter-onset conditions are affected by the locations of the cutting tool relative to the workpiece and the geometry of the workpiece. The chatter frequency is just above the fundamental natural frequency of the shaft and varies with the spin rate. The results obtained for four uniform workpieces are in excellent agreement with the experimental results available in the literature.

## REFERENCES


1. M. E. MERCHANT 1944 *Journal of Applied Mechanics* **66**, 168–175. Basic mechanics of the metal cutting process.
2. E. H. LEE and B. W. SHAFFER 1951 *Journal of Applied Mechanics* **73**, 405–413. The theory of plasticity applied to a problem of machining.
3. D. W. WU and C. R. LIU 1985 *Journal of Engineering for Industry* **111**, 112–118. An analytical model of cutting dynamics, Part 2: verification.
4. I. E. MINIS and A. TEMBO 1993 *Journal of Engineering for Industry* **115**, 9–14. Experimental verification of a stability theory for periodic cutting operations.
5. H. E. MERRITT 1965 *Journal of Engineering for Industry* **87**, 447–454. Theory of self-excited machine tool chatter.
6. S. KATO and E. MARUI 1974 *Journal of Engineering for Industry* **96**, 179–186. On the cause of regenrerative chatter due to workpiece deflection.
7. T. KANEKO, H. SATO, Y. TANI and M. O-HORI 1984 *Journal of Engineering for Industry* **106**, 222–228. Self-excited chatter and its marks in turning.
8. B. E. KLAMECKI 1989 *Journal of Engineering for Industry* **111**, 193–198. On the effects of turning process asymmetry on process dynamics.
9. W. F. LU and B. E. KLAMECKI 1990 *Proceedings*, *ASME WAM*, *PED*, Vol. 44, 237–252. Prediction of chatter onset in turning with a modified chatter model.
10. S. C. LIN 1990 *Annals of CIRP* **44**, 253–265. A method to analyze the stability of machine tool.
11. C.-C. HWANG, R.-F. FUNG and J.-S. LIN 1997 *Journal of Sound and Vibration* **203**, 363–372. Strong non-linear dynamics of cutting processes.
12. C. H. CHEN, K. W. WANG and Y. C. SHIN 1994 *Journal of Vibration and Acoustics* **116**, 506–513. An integrated approach toward the dynamic analysis of high-speed spindles. Part 1: system model.
13. C. H. CHEN, K. W. WANG and Y. C. SHIN 1994 *Journal of Vibration and Acoustics* **116**, 514–522. An integrated approach toward the dynamic analysis of high-speed spindles. Part 2: dynamic under moving end load.
14. Z. C. WANG, W. L. CLEGHORN and S. D. YU 1999 *Proceeding of the* 1999 *ASME Design Engineering Technical Conferences*, *Las Vegas*, *Nevada*. Chatter in turning process incorporating the effect of ploughing force.
15. J. W.-Z. ZU and R. P. S. HAN 1994 *Transactions of American Society of Mechanical Engineers Journal of Applied Mechanics* **61**, 152–159. Dynamic response of a spinning Timoshenko beam with general boundary conditions and subjected to a moving load.
16. C. W. LEE, R. KATZ, A. G. ULSOY and R. A. SCOTT 1988 *Journal of Sound and Vibration* **122**, 119–130. Modal analysis of a distributed parameter rotating shaft.
17. W. F. LU 1990 *Ph.D. Thesis*, *University of Minnesota*. Prediction of chatter onset in turning process with a new process model.